

## Approximating spatially exclusive invasion processes

Joshua V. Ross\* and Benjamin J. Binder

*School of Mathematical Sciences, University of Adelaide, South Australia, 5005 Australia*

(Received 28 January 2014; revised manuscript received 6 April 2014; published 15 May 2014)

A number of biological processes, such as invasive plant species and cell migration, are composed of two key mechanisms: motility and reproduction. Due to the spatially exclusive interacting behavior of these processes a cellular automata (CA) model is specified to simulate a one-dimensional invasion process. Three (independence, Poisson, and 2D-Markov chain) approximations are considered that attempt to capture the average behavior of the CA. We show that our 2D-Markov chain approximation accurately predicts the state of the CA for a wide range of motility and reproduction rates.

DOI: [10.1103/PhysRevE.89.052709](https://doi.org/10.1103/PhysRevE.89.052709)

PACS number(s): 87.17.-d, 87.18.-h, 87.85.-d

### I. INTRODUCTION

Spatially exclusive invasion processes are commonly found in biological systems, including invasive plant species [1–6] and tissue growth and cell migrations [7–12]. The two main mechanisms that primarily drive the evolution of these physical systems are motility and reproduction. For example, seed dispersal and cell movement are motility mechanisms, and clonal root propagation and cell proliferation are reproduction mechanisms. Developing mathematical models incorporating motility and reproduction mechanisms provides a means to understand and predict important invasion processes, such as the threat to biodiversity by invasive plant species and the growth of cancerous tumors.

Cellular automata (CA) or agent-based models have been implemented to simulate plant invasion and monolayer cell processes [1,5–8,11,12], and in this work we focus on modeling an invasion front propagating in just a single spatial direction. One example of where unidirectional invasion fronts occur is in scratch assays [13–15], a cell-based experiment often used to estimate the rates of cell motility and proliferation (see Fig. 1). Another example is the agent-based modeling of invasive pine trees from commercial plantations into natural habitats [6]. The CA framework consists of occupied sites on a lattice (agents) that represent individuals (e.g., plants or cells), and at any given time each site can only be occupied by a single agent, which is a spatial exclusion process [16,17]. We specify continuous-time and one-dimensional discrete space CA rules to simulate the motility and reproduction mechanisms in the invasion process [18].

The CA model simulates the spatially exclusive and stochastic interactive behavior of individuals within the invasion process, allowing for the effect of spatial structuring to be explicitly accounted for in the system. In contrast, the derivation of classical continuum models that predict the collective dynamics of the evolving population [19–23] assume spatial homogeneity or the mean-field assumption [24–26]. It is well known that in a one-dimensional Cartesian geometry the classical continuum model is a reaction-diffusion equation, with diffusivity  $D$  (motility coefficient) and reproduction rate  $\lambda$ ,

and under certain conditions the invasion front advances with speed  $s = \sqrt{2D\lambda}$  [21]. However, many choices of  $D$  and  $\lambda$  give the same wave speed and even matching the wave front to experimental or simulation data does not uniquely determine the rates of motility and reproduction in the system [8]. This motivates us to derive approximations for averaged CA properties to predict the collective motion of the invasion process.

We consider two existing approximations (called the independence approximation and the Poisson approximation, respectively), and a third new approximation (called the 2D-Markov chain approximation) is introduced to approximate the averaged CA behavior.

The first approximation—the independence approximation—assumes independence (i.e., the mean-field assumption) between the occupancy of sites in the CA model. It has been shown that in the absence of reproduction this approximation provides the exact marginal probabilities of occupancy [18]. Numerous approximations which have been considered in the literature, mostly of the partial differential equation continuum type, are further approximations to this model [17,18,27–30]. Consistent with the findings of these studies, the independence approximation is shown to be accurate only when the rate of reproduction is at least two orders of magnitude smaller than the rate of motility.

By considering the case of reproduction in the absence of motility, the occupancy can be described explicitly by the Poisson process [31,32]. This forms the basis of the second approximation—the Poisson approximation—when both reproduction and motility mechanisms are present in the system, and we show that the approximation becomes increasingly inaccurate as the rate of motility increases for a fixed rate of reproduction.

We derive an approximation—the 2D-Markov chain approximation—which is a Markov chain of much lower dimension than the original CA exclusion process. We find that this last approximation accurately predicts the state of the invasion process provided the motility rate is less than two orders of magnitude of that of the reproduction rate. This 2D-Markov chain approximation provides an accurate approximation in systems with moderate to high rates of reproduction, for example as is the case for breast cancer cell migrations where cell motility and cell proliferation rates are estimated to be of the same order [7], and invasive plant

\*joshua.ross@adelaide.edu.au

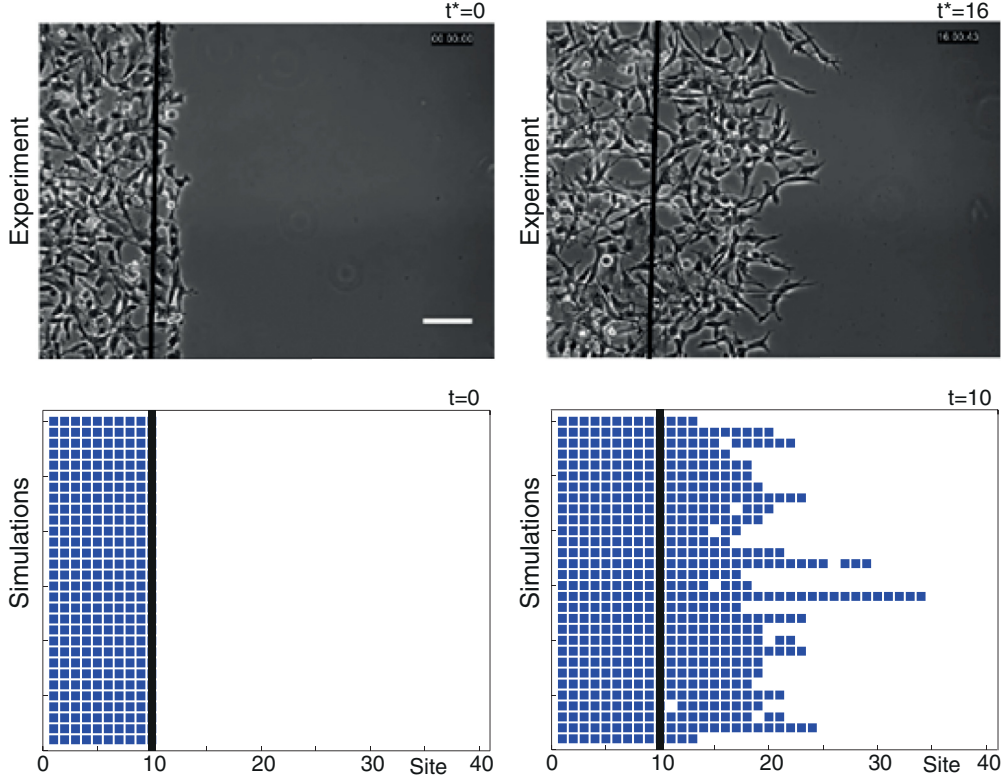


FIG. 1. (Color online) Cell invasion assay. Top: Modified images of an experiment (reprinted from PLoS ONE, Yu and Machesky [14], under the terms of the Creative Commons Attribution License). The time  $t^*$  is in hours. Bottom: Thirty CA simulations, with reproduction rate  $\lambda_r = 1$ , motility rate  $\lambda_m = 1$ , initial condition  $x_0 = 10$  (black line), and lattice length  $L = 250$ . The blue (gray) squares illustrate the sites that are occupied.

species (e.g., *Carpobrotus affine acinaciformis*) that reproduce primarily through clonal root propagation [5].

## II. CELLULAR AUTOMATA MODEL

We specify a continuous-time, discrete space CA model to simulate the motility and reproduction mechanisms in a spatially exclusive invasion process evolving in one spatial dimension [18]. We consider a nondimensional single row lattice of unit spacing with  $L$  sites, each of which may be occupied by an agent (e.g., plant or cell). Each agent or site that is occupied attempts to move at rate  $\lambda_m$ ; the direction of this movement—left or right—is chosen with equal probability, and the move only proceeds if the site in the chosen direction is unoccupied. A successful motility event results in the agent moving site. Similarly, each agent attempts to proliferate at rate  $\lambda_r$ ; the direction of reproduction—left or right—is chosen with equal probability, and the event only proceeds if the site in the chosen direction is unoccupied. A successful reproduction event results in an extra site, in the chosen direction, becoming occupied. For all the simulations we initially populate all the sites with agents to the left of and including  $x_0$ , where  $1 \leq x_0 \leq L$ . Thirty CA simulations are illustrated with blue (gray) squares for occupied sites in Fig. 1 (bottom).

This spatially exclusive invasion process is a continuous-time Markov chain [33]. We denote the random state of the chain at time  $t$  by  $X(t)$ , which is a binary vector of length  $L$ , the maximum number of agents possible, where the  $i$ th element of the vector is zero if site  $i$  is not occupied by

a cell, and is one if site  $i$  is occupied by a cell. The process has the transition rates shown in Table I where  $x_i(t)$  is the state of site  $i$  at time  $t$  and  $e_i$  is a vector of length  $L$  with a one in the  $i$ th position and zeros elsewhere. The size of the state space of this Markov chain is then  $\sum_{x=x_0}^L \binom{L}{x}$  where  $x_0$  is the initial number of agents.

The distribution of the state of the exclusion process at any time  $t$  may be evaluated by solving the forward equation [33]. However, this is practically infeasible for anything other than systems with small  $x_0$  and  $L$ . Realizations of the exclusion process are generated by exploiting the sample path behavior of the process [34–36] (last row, Fig. 1). We now consider the

TABLE I. The transitions and associated rates which define the stochastic exclusion process of the CA model.

Event	Transition $x(t) \rightarrow$	Rate
Motility right $i = 2, \dots, L$	$x(t) + e_i - e_{i-1}$	$\frac{\lambda_m}{2} x_{i-1}(t)[1 - x_i(t)]$
Motility left $i = 1, \dots, L - 1$	$x(t) + e_i - e_{i+1}$	$\frac{\lambda_m}{2} x_{i+1}(t)[1 - x_i(t)]$
Reproduction $i = 2, \dots, L - 1$	$x(t) + e_i$	$\frac{\lambda_r}{2} [1 - x_i(t)] [x_{i-1}(t) + x_{i+1}(t)]$
Reproduction site 1	$x(t) + e_1$	$\frac{\lambda_r}{2} [1 - x_1(t)] x_2(t)$
Reproduction site $L$	$x(t) + e_L$	$\frac{\lambda_r}{2} [1 - x_L(t)] x_{L-1}(t)$

three approximations to this stochastic process. The aim is to evaluate the probabilities  $p_i(t)$ , being the marginal probability that site  $i$  is occupied at time  $t$ , for  $i = 1, \dots, L$ .

### III. INDEPENDENCE APPROXIMATION

Assuming independence between occupied sites gives rise to the system of  $L$  ordinary differential equations (ODEs):

$$\frac{dp_i}{dt} = \frac{\lambda_m}{2} (p_{i-1} - 2p_i + p_{i+1}) + \frac{\lambda_r}{2} (1 - p_i)(p_{i-1} + p_{i+1}),$$

for  $i = 2, \dots, L - 1$ ,

$$\frac{dp_1}{dt} = -\frac{\lambda_m}{2} p_1 + \frac{\lambda_m}{2} p_2 + \frac{\lambda_r}{2} p_2 (1 - p_1),$$

and

$$\frac{dp_L}{dt} = -\frac{\lambda_m}{2} p_L + \frac{\lambda_m}{2} p_{L-1} + \frac{\lambda_r}{2} p_{L-1} (1 - p_L),$$

for the marginal probabilities of occupancy. This is called the independence approximation. Note that in the case of motility only with  $\lambda_r = 0$  it has been shown that the approximation gives the true marginal probabilities of occupancy [18]. Several approximations appearing in the literature are based upon this approximation [17,18,27–30].

### IV. POISSON APPROXIMATION

For the second approximation we begin by considering the case of reproduction only with  $\lambda_m = 0$ . The distribution of the exclusion process may be found explicitly. This is because the agent initially at site  $x_0$  moves to the right at constant rate  $\lambda_r/2$ , and all cells to the left of the rightmost occupied site must be occupied [32]. Hence, the probability of the rightmost site occupied at time  $t$  being site  $i$ ,  $q_i(t)$ , is given by the system of ODEs ([31,32]) (corresponding to the Poisson process in the limit  $L \rightarrow \infty$ ):

$$\frac{dq_i(t)}{dt} = \frac{\lambda_r}{2} q_{i-1}(t) - \frac{\lambda_r}{2} q_i(t), \quad i = x_0, \dots, L - 1,$$

with  $q_i(t) = 0$  for  $i = 1, \dots, x_0 - 1$  and

$$\frac{dq_L(t)}{dt} = \frac{\lambda_r}{2} q_{L-1}(t).$$

The marginal probabilities of occupancy are then given exactly by

$$p_i(t) = \sum_{j=i}^L q_j(t) = 1 - \sum_{j=1}^{i-1} q_j(t), \quad i = 1, \dots, L,$$

since site  $i$  is occupied if the rightmost occupied site is position  $i$  or to the right of position  $i$ .

We replace  $\lambda_r/2$  in the above with  $(\lambda_r + \lambda_m)/2$  to provide an approximation to the combined motility and reproduction exclusion process.

### V. 2D-MARKOV CHAIN APPROXIMATION

The 2D-Markov chain approximation builds upon the exact correspondence between the CA process and the Poisson process in the absence of motility. In the case of reproduction only, knowledge of the rightmost site occupied is sufficient

TABLE II. The transitions and associated rates which define the 2D-Markov chain approximation.

Event	Transition $(r(t), g(t)) \rightarrow$	Rate
Motility right	$(r(t) + 1, g(t) + 1)$	$\frac{\lambda_m}{2} 1_{r(t) < L}$
Motility left	$(r(t) - 1, g(t) - 1)$	$\frac{\lambda_m}{2} g(t) b(0, r(t), \lambda_r, \lambda_m)$
Reproduction right	$(r(t) + 1, g(t))$	$\frac{\lambda_r}{2} 1_{r(t) < L}$
Reproduction other	$(r(t), g(t) - 1)$	$\frac{\lambda_r}{2} \left[ 2g(t) \frac{r(t)-g(t)-1}{r(t)+g(t)-1} + b(0, r(t), \lambda_r, \lambda_m) 1_{g(t) > 0} \right]$

to fully characterize the system. Once motility is present, this is not the case as gaps (i.e., unoccupied sites between occupied sites) are likely to appear, and hence there is the possibility of movement or reproduction into these vacant sites. We approximate the position of the rightmost site occupied and the number of gaps at time  $t$  and use ansatze for how the gaps are spread between site 1 and the rightmost occupied site.

Consider a bivariate continuous-time Markov chain  $X(t) = (R(t), G(t))$ , where  $R(t)$  is the position of the rightmost occupied site and  $G(t)$  is the number of unoccupied sites to the left of the rightmost occupied site at time  $t$ . The number of occupied sites is therefore  $R(t) - G(t)$ . We use  $(r(t), g(t))$  to denote the realized state of this chain at time  $t$ . The 2D-Markov chain approximation has the transition rates shown in Table II.

The first event type which changes the state of the chain is motility to the right by the rightmost occupied site—labeled *Motility right* in Table II. This increases the rightmost occupied site by one and also increases the number of gaps by one as there is now an additional gap to the left of the rightmost occupied site. The rate of this event is  $\lambda_m/2$  provided the rightmost occupied site is not in position  $L$  (in Table II,  $1_c$  is the indicator function which equals one if  $c$  is true and is equal to zero otherwise).

Similarly, reproduction to the right by the rightmost occupied site—labeled *Reproduction right* in Table II—increases the rightmost occupied site by one but does not result in an increase in the number of gaps. The rate of this event is  $\lambda_r/2$ , once again provided that the rightmost occupied site is not in position  $L$ .

The only way the rightmost occupied site can decrease is by a motility event of the rightmost occupied site into a gap to its immediate left—labeled *Motility left* in Table II. Hence, the rate of this event in our approximate model is  $\lambda_m/2$  multiplied by the probability that the site immediately to the left of the rightmost occupied site is vacant. If gaps were uniformly distributed between site 1 and the rightmost occupied site, then the required probability would be  $g(t)/(r(t) - 1)$ . However, as motility is required to produce gaps, and in turn a motility event requires a gap to occur, it is consequently more likely that such events occur at occupied sites closer to site  $r(t)$  than site 1; to be emphatic, the rightmost occupied site always has a vacant site to its right unless it is in site  $L$ . With the same reasoning, it can be seen that the probability of site  $[r(t) - 1]$  being vacant will be more likely when reproduction is large relative to motility for a fixed number of gaps, whereas when motility becomes very large the occupied sites (and hence gaps) will be close to

uniformly spread between site 1 and site  $r(t)$ . To account for this higher probability of vacancy in the position immediately to the left of the rightmost occupied site and its dependence on reproduction rate relative to motility rate, we use the ansatz

$$b(0, r(t), \lambda_r, \lambda_m) = \frac{f(0, \frac{\lambda_r}{\lambda_r + \lambda_m})}{F(r(t) - 1, \frac{\lambda_r}{\lambda_r + \lambda_m})},$$

where  $f(0, p)$  is the geometric probability mass function of no failures with probability of failure  $p$ , and  $F(x, p)$  is the corresponding cumulative distribution function of  $x$  failures. The resulting rate of this event is therefore denoted  $(\lambda_m/2)g(t)b(0, r(t), \lambda_r, \lambda_m)$ , being the rate of migration to the left multiplied by our approximation for the probability of site  $r(t) - 1$  being unoccupied at time  $t$ .

The final event which changes the state of the chain is when reproduction results in the removal of a gap—labeled *Reproduction other* in Table II. This occurs if the rightmost occupied site reproduces into a vacant site to its immediate left, or if any other site reproduces into any of their vacant neighboring sites. We decompose this rate into these types of “events”; the former is specified in an identical way to the *Motility left* rate just described and hence occurs with rate  $(\lambda_r/2)g(t)b(0, r(t), \lambda_r, \lambda_m)$ , while the latter requires another ansatz as we will now derive. The rate of the second group of events—reproduction into any neighboring vacant site by all of the  $r(t) - g(t)$  sites excluding the rightmost occupied site—is  $\lambda_r/2$  times the number of unoccupied-occupied pairs that exist, excluding any involving the rightmost site. We use the ansatz  $2g(t)\{[r(t) - g(t) - 1]/[r(t) + g(t) - 1]\}$  to approximate the number of such pairs. To assist in understanding this ansatz, consider the case  $r(t) = 6$ , at some arbitrary time  $t$ , with different numbers of gaps,  $g(t)$ : if  $g(t) = 0$ , then the number of unoccupied-occupied pairs is zero, as reflected in our ansatz; if  $g(t) = r(t) - 1$ , the maximum possible number of gaps under any scenario, then the number of unoccupied-occupied pairs excluding the rightmost occupied site is once again zero, which is also reflected in our ansatz. Now consider a case with a small number of gaps, say  $g(t) = 1$ ; then if this gap was allocated uniformly at random, there exists two realizations giving rise to one unoccupied-occupied pair and three realizations giving rise to two unoccupied-occupied pairs, and hence under this assumption the average number of unoccupied-occupied pairs is  $8/5 \approx 1.6$ ; using our ansatz, the number of unoccupied-occupied pairs is evaluated as  $8/6 \approx 1.33$ . The lower value used here accounts for the earlier noted property that the gap is more likely to be at site  $r(t) - 1$  and hence reduces the average number of unoccupied-occupied pairs. As  $g(t)$  increases, the above considerations also motivate and support the chosen ansatz.

It can be seen that the approximation just described is a Markov chain with only two dimensions, being the position of the rightmost occupied site and the number of gaps, respectively. Here, the state space is  $\{(r, g) : x_0 \leq r \leq L, 0 \leq g \leq r - x_0\}$ . This should be compared with the original Markov chain exclusion process, where the number of states is  $\sum_{x=x_0}^L \binom{L}{x}$ . Hence, the 2D-Markov chain is much simpler to handle. To evaluate the marginal probabilities of occupancy, we use the `mexpv.m` function in the `EXPOKIT` package for `MATLAB`<sup>TM</sup>. Given the probability of

each state  $p_{r,g}(t)$ —the probability the rightmost agent at time  $t$  is in position  $r$  and there exist  $g$  unoccupied sites to the right of this agent at time  $t$ —we may approximate the marginal probability of occupancy by

$$p_i(t) = 1 - \sum_{r=x_0}^{i-1} \sum_{g=0}^{r-x_0} p_{r,g}(t) - \sum_{r=i+1}^L \sum_{g=0}^{r-x_0} p_{r,g}(t) \times g \times b(r - i - 1, r, \lambda_r, \lambda_m),$$

for  $i = 1, \dots, L$ , where

$$b(r - i - 1, r(t), \lambda_r, \lambda_m) = \frac{f(r - i - 1, \frac{\lambda_r}{\lambda_r + \lambda_m})}{F(r(t) - 1, \frac{\lambda_r}{\lambda_r + \lambda_m})}$$

for  $i = 1, \dots, r(t) - 1$  is the earlier used ansatz extended to the other sites in the lattice. The equation for  $p_i(t)$  may be read as one minus the probability of not being occupied, where site  $i$  is not occupied if either the rightmost cell is to the left of site  $i$  or if the rightmost cell is to the right of site  $i$  but site  $i$  is unoccupied.

We note that the 2D-Markov chain approximation reduces to the Poisson process in the case of reproduction only (i.e., when  $\lambda_m = 0$ ). Also, our 2D-Markov chain approximation shares some common features with the *one-hole approximation* [31,32,37]. In the one-hole approximation it is assumed that only a single unoccupied site exists behind the rightmost occupied site, and via a particular ansatz a one-dimensional approximation can be derived [31,32,37]. While weakening slightly the assumptions of the Poisson process approximation, this one-hole approximation obviously still requires reproduction to be much larger than motility to provide an accurate approximation [37]. In comparison, our approximation, while requiring two dimensions, allows for any number of gaps to emerge and instead uses ansätze for how these gaps are distributed behind the rightmost occupied site.

## VI. DISCUSSION

Shown in Fig. 2 is the average invasion wave profile or estimate of marginal probabilities (solid black curves) from 10 000 CA simulations, and the three approximations: independence approximation (broken black curves), Poisson approximation (solid gray curves), and 2D-Markov chain approximation (broken gray curves). All the results are for the same initial condition  $x_0 = 2$  and reproduction rate  $\lambda_r = 1$ . The effect of increasing both the motility rate  $\lambda_m$  (top–bottom) and time  $t$  (left–right) is shown in the panels. As expected, we see (top row) that in the case of reproduction only when  $\lambda_m = 0$  the Poisson and 2D-Markov chain approximation are an excellent match to the averaged CA data, but the independence approximation increasingly overestimates advancement of the CA wave profile with time (left–right). For increasing rate of motility (top–bottom) we find that the Poisson approximation increasingly deviates from the CA data, while the 2D-Markov chain approximation still accurately predicts the collective motion of the system for moderate values of  $\lambda_m$  (second and third row). The independence approximation provides the best estimate of the invasion process for the largest value of the motility rate (last row).

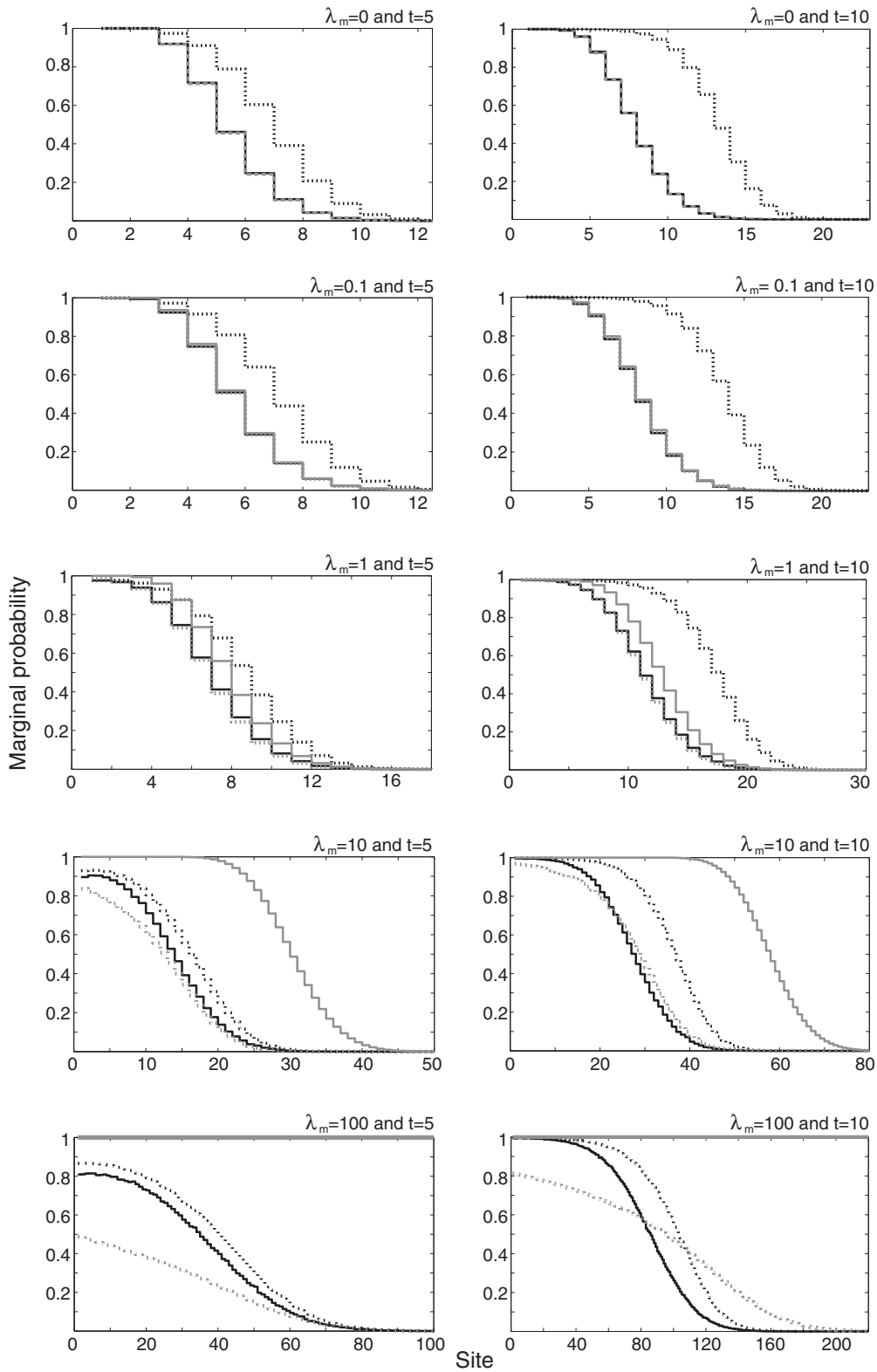


FIG. 2. Comparison of the three approximations to averaged CA data from 10 000 simulations (solid black curves), with reproduction rate  $\lambda_r = 1$ , initial condition  $x_0 = 2$ , and domain length  $L = 250$ . Independence approximation (broken black curves), Poisson approximation (solid gray curves), and 2D-Markov chain approximation (broken gray curves). Note that the curves are indistinguishable in some of the panels, and in the last row the values for the Poisson approximation (solid gray curves) are close to unity. The results illustrate the differences between the approximations and averaged CA data for both increasing time  $t$  (left–right) and motility rate  $\lambda_m$  (top–bottom).

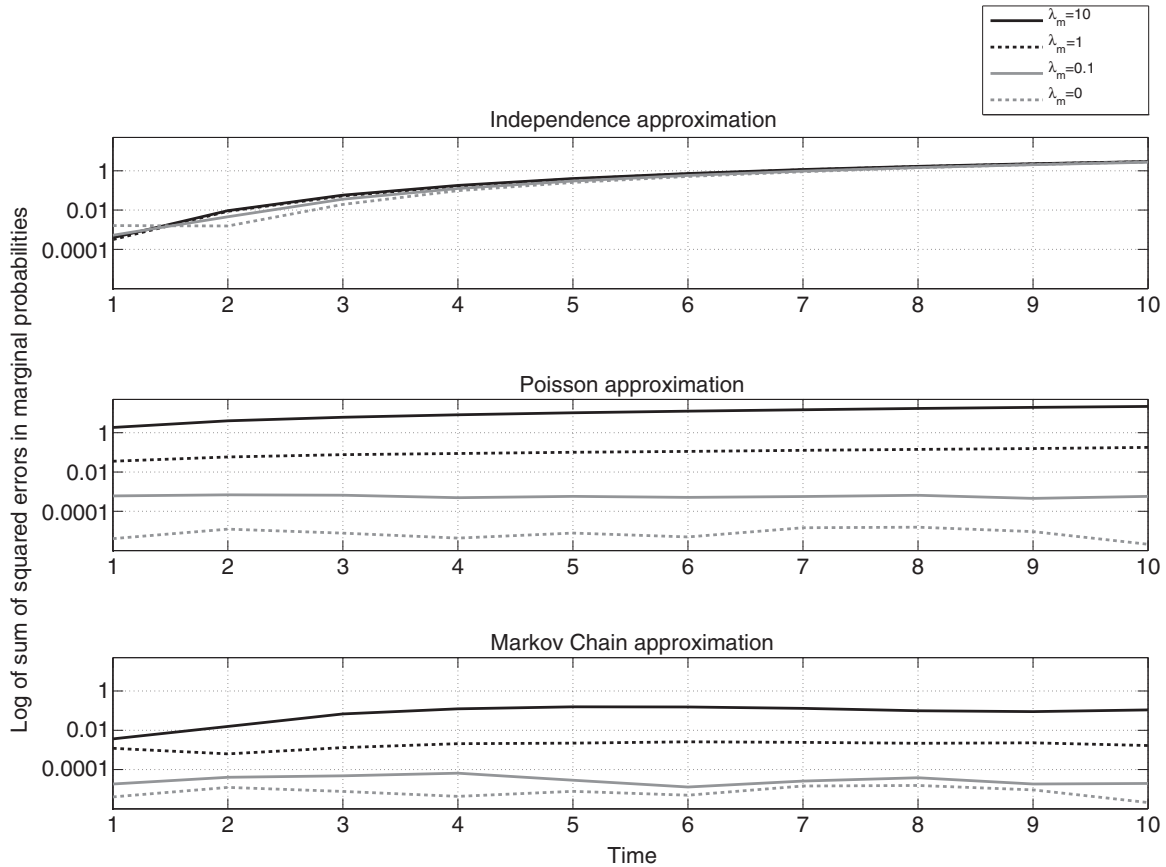


FIG. 3. Accuracy of the three approximations as measured by the sum of squared errors of marginal probabilities in comparison to averaged CA data evaluated from 100 000 simulations, with reproduction rate  $\lambda_r = 1$ , initial condition  $x_0 = 2$ , domain length  $L = 250$ , and  $\lambda_m = \{0, 0.1, 1, 10\}$ . The results illustrate that the Markov chain approximation is more accurate than the other two approximations, for nearly all integer values of the time  $t$ .

In Fig. 3 we present the sum of squared errors in marginal probabilities of occupancy for the independence approximation (top), the Poisson approximation (middle), and the 2D-Markov chain approximation (bottom) across a wider range of times,  $t = 1$  to 10 in units of one, for motility rates  $\lambda_m = 0, 0.1, 1$ , and 10. The *true* marginal probability was estimated based upon 100 000 simulations. It can be seen that for all motility rates less than the reproduction rate the 2D-Markov chain approximation provides the best approximation uniformly with respect to time and that this approximation is highly accurate. When the motility rate is equal to or exceeds the reproduction rate, the independence approximation is better for earlier times, with the 2D-Markov chain still being the best approximation for later times.

The accuracy can be easily inferred for other motility and reproduction rates, as the behavior and hence accuracy are only dependent upon the ratio (with appropriate scaling of time) and the accuracy is monotonically decreasing with increasing motility rate. We also investigated a range of initial conditions,  $x_0$ , which did not affect the accuracy of the 2D-Markov chain approximation.

In this work we have developed a 2D-Markov chain approximation to a spatially exclusive invasion process, which

is accurate over several different orders of magnitude of motility rate to reproduction rate. We have demonstrated that it provides an excellent prediction of the collective motion of individuals when the reproduction rate is of the same order as the motility rate, as observed, for example, in breast cancer cell migrations [7]. Approximations proposed hitherto that have assumed the spatial independence between individuals in the process require the rate of reproduction to be at least two orders of magnitude smaller than the rate of motility to accurately predict the frontal expansion of the invading population [17,18,27–30]. This Markov chain representation of the exclusion system, which is much lower dimensional than the original description, opens up the opportunity to increase the efficiency of statistical estimation procedures, which aim to estimate motility and reproduction rates based upon time-lapse image data [7,8].

However, a challenge still remains, as the approximation does break down once the motility rate is at least one order of magnitude larger than the reproduction rate (fourth and fifth row, Fig. 2; bottom of Fig. 3). It is known that the independence approximation will become accurate, at least for sufficiently early times, as the motility rate becomes much larger than the reproduction rate, as it is exact in the case where there is motility only [18]. An approximation which

fills the void between these cases is now the main focus of research in this area. The extension of the 2D-Markov chain approximation to handle both higher-dimensional spaces and multispecies dynamics is also left to future research.

#### ACKNOWLEDGMENTS

This research was supported under the Australian Research Council's Discovery Projects funding scheme (Project No. DP110102893) and National Health and Medical Research Scheme (Project No. APP1069757).

- 
- [1] N. Nehrbaas and E. Winkler, *Ecol. Modelling* **210**, 377 (2007).
- [2] R. A. Wadsworth, Y. C. Collingham, S. G. Willis, B. Huntley, and P. E. Hume, *J. Appl. Ecol.* **37**, 28 (2000).
- [3] P. Pysek and K. Prach, *J. Biogeogr.* **20**, 413 (1993).
- [4] J. A. Kemperan and B. V. Barnes, *Can. J. Botany* **54**, 2603 (1976).
- [5] T. Sintes, E. Moragues, and A. Traveset, *J. Rita. Ecol. Modelling* **206**, 110 (2007).
- [6] S. I. Higgins, D. M. Richardson, and R. M. Cowling, *Ecology* **77**, 2043 (1996).
- [7] M. J. Simpson, B. J. Binder, P. Haridas, B. K. Wood, K. K. Treloar, D. L. S. McElwain, and R. E. Baker, *Bull. Math. Biol.* **75**, 871 (2013).
- [8] M. J. Simpson, K. K. Treloar, B. J. Binder, P. Haridas, K. J. Manton, D. I. Leavesley, D. L. S. McElwain, and R. E. Baker, *J. Roy. Soc. Interface* **10**, 20130007 (2013).
- [9] B. J. Binder, K. A. Landman, M. J. Simpson, M. Mariani, and D. F. Newgreen, *Phys. Rev. E* **78**, 031912 (2008).
- [10] B. J. Binder and K. A. Landman, *J. Theor. Biol.* **259**, 541 (2009).
- [11] D. Zhang, I. M. Brinas, B. J. Binder, K. A. Landman, and D. F. Newgreen, *Dev. Biol.* **339**, 280 (2010).
- [12] B. J. Binder, K. A. Landman, D. F. Newgreen, J. E. Simkin, Y. Takahashi, and D. Zhang, *Bull. Math. Biol.* **74**, 474 (2012).
- [13] H.-H. Ryu, S. Jung, T.-Y. Jung, K.-S. Moon, I.-Y. Kim, Y.-I. Jeong, S.-G. Jin, J. Pei, M. Wen, and W.-Y. Jang, *Int. J. Oncol.* **41**, 1305 (2012).
- [14] X. Yu and L. M. Machesky, *PLoS ONE* **7**, e30605 (2012).
- [15] S. Zheng, J. Huang, K. Zhou, C. Zhang, Q. Xiang, Z. Tan, T. Wang, and X. Fu, *PLoS ONE* **6**, e22439 (2011).
- [16] D. Chowdhury, A. Schadschneider, and K. Nishinari, *Phys. Life. Rev.* **2**, 318 (2005).
- [17] M. J. Simpson, K. A. Landman, and B. D. Hughes, *Physica A* **389**, 3779 (2010).
- [18] K. J. Davies, J. E. F. Green, N. G. Bean, B. J. Binder, and J. V. Ross, *Math. Biosci.*, doi:10.1016/j.mbs.2014.04.004.
- [19] P. K. Maini, D. L. S. McElwain, and D. I. Leavesley, *Tissue Eng.* **10**, 475 (2004).
- [20] P. K. Maini, D. L. S. McElwain, and D. Leavesley, *Appl. Math. Lett.* **17**, 575 (2004).
- [21] J. D. Murray, *Mathematical Biology I: An Introduction*, 3rd ed. (Springer-Verlag, Heidelberg, 2002).
- [22] B. G. Sengers, C. P. Please, and R. O. C. Oreffo, *J. Roy. Soc. Interface* **4**, 1107 (2007).
- [23] J. A. Sherratt and J. D. Murray, *Proc. R. Soc. London B* **241**, 29 (1990).
- [24] M. Raghob, N. A. Hill, and U. Dieckmann, *J. Math. Biol.* **62**, 605 (2011).
- [25] U. Dieckmann, R. Law, and J. A. J. Metz, *The Geometry of Ecological Interactions: Simplifying Spatial Complexity* (Cambridge University Press, Cambridge, 2000).
- [26] R. Law, D. J. Murrel, and U. Dieckmann, *Ecology* **84**, 252 (2003).
- [27] C. Deroulers, M. Aubert, M. Badoual, and B. Grammaticos, *Phys. Rev. E* **79**, 031917 (2009).
- [28] C. J. Penington, B. D. Hughes, and K. A. Landman, *Phys. Rev. E* **84**, 041120 (2011).
- [29] C. J. Penington, K. Korvasová, B. D. Hughes, and K. A. Landman, *Phys. Rev. E* **86**, 051909 (2012).
- [30] M. J. Plank and M. J. Simpson, *J. Roy. Soc. Interface* **9**, 2983 (2012).
- [31] M. Bramson, P. Calderoni, A. De Masi, P. Ferrari, J. Lebowitz, and R. H. Schonmann, *J. Stat. Phys.* **45**, 5 (1986).
- [32] T. Callaghan, E. Khain, L. M. Sander, and R. M. Ziff, *J. Stat. Phys.* **122**, 5 (2006).
- [33] J. R. Norris, *Markov Chains* (Cambridge University Press, Cambridge, 1997).
- [34] M. S. Bartlett, *J. Roy. Stat. Soc. C* **2**, 44 (1953).
- [35] D. T. Gillespie, *J. Phys. Chem.* **81**, 2340 (1977).
- [36] D. G. Kendall, *J. Roy. Stat. Soc. B* **12**, 116 (1950).
- [37] D. C. Markham, M. J. Simpson, P. K. Maini, E. A. Gaffney, and R. E. Baker, *J. Theor. Biol.* **353**, 95 (2014).